Alkyne Coupling Reactions Mediated by Organolanthanides. Probing the Mechanism by Metal and Alkyne Variation

Craig M. Forsyth, Steven P. Nolan, Charlotte L. Stern, and Tobin J. Marks*

Department of Chemistry, Northwestern University, Evanston, Illinois 60208-3113

Arnold L. Rheingold

Department of Chemistry, University of Delaware, Newark, Delaware 19716

Received March 23, 1993

This contribution addresses, using the non-redox-active ion La^{3+}, the constraints under which lanthanide M—C≡CR functionalities undergo facile coupling to yield binuclear $M_2(\mu\text{-}RC_4R)$ complexes. The reaction of $Cp'_2LaCHTMS_2$ ($Cp' = \eta^5\text{-}Me_5C_5$) with PhCCH at room temperature yields the coupled product $(Cp'_2La)_2(\mu\text{-}PhC_4Ph)$ (monoclinic space group $C2/m$, a = 15.600(2) Å, b = 14.318(2) Å, c = 15.368(2) Å, β = 114.17(1)°, Z = 2, R = 0.050, R_w = 0.063) plus CH_2TMS_2. Reaction of $Cp'_2LaCHTMS_2$ with t-BuCCH at 0 °C, yields the uncoupled dimer $(Cp'_2LaC_2\text{-}t\text{-}Bu)_2$ (plus CH_2TMS_2), which, in toluene solution at 50 and 60 °C, undergoes clean unimolecular conversion to the coupled dimer $(Cp'_2La)_2(\mu\text{-}t\text{-}BuC_4\text{-}t\text{-}Bu)$ (monoclinic space group $P2_1/n$, a = 11.232(2) Å, b = 14.199(3) Å, c = 15.309(4) Å, β = 103.35(2)°, Z = 2, R = 0.027, R_w = 0.034). These results argue that excursions in formal metal oxidation state (+3 ⇌ +2) are not important along the reaction coordinate, that acetylene aryl substituents are not necessary for the coupling process to occur, and that the immediate kinetic precursor to the coupled product is an uncoupled dimer.

Carbon–carbon bond-forming reactions comprise an integral part of both stoichiometric and catalytic metal-assisted organic synthesis. For organo-f-element complexes in homogeneous solution, the great preponderance of such transformations involving unsaturated, unfunctionalized hydrocarbon molecules proceeds via insertive pathways (e.g., eq 1) in which there is no change in formal

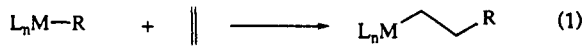

(1)

metal oxidation state.[1] Cases where the metal undergoes a +1 change in oxidation state are more rare (e.g., eq 2).[2,3] To our knowledge, no well-documented examples of such processes exist where the f-element center undergoes analogous ±2 changes in formal oxidation state.

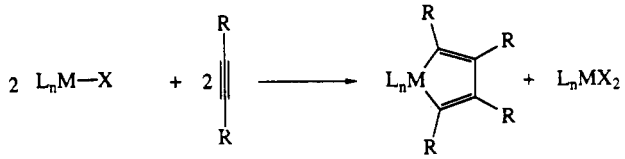

We recently reported a thermochemical investigation of a series of Cp'_2SmR/Cp'_2SmX compounds ($Cp' = \eta^5$-Me_5C_5) where R, X = hydrocarbyl, hydride, amino, halo, etc.[3] This included the synthesis of a number of new compounds, calorimetric measurements, and a thermodynamic analysis of a number of known or hypothetical transformations. Of the complexes reported, one (**1**) was prepared by a fairly general approach to acetylide complexes of electropositive metals (eq 3, TMS = $SiMe_3$) and

$$2Cp'_2SmCHTMS_2 + 2PhC{\equiv}CH \rightarrow \underset{\mathbf{1}}{(Cp'_2Sm)_2(C_2Ph)_2} + 2CH_2TMS_2 \quad (3)$$

was characterized by ^1H NMR, cryoscopy, elemental analysis, and infrared spectroscopy. By analogy to crystallographically characterized $(Cp_2Er\text{-}\mu\text{-}C_2\text{-}t\text{-}Bu)_2$ (**2**),[4] $[(MeC_5H_4)_2Sm\text{-}\mu\text{-}C_2\text{-}t\text{-}Bu]_2$ (**3**),[5] and $[Cp'(THF)_2Eu\text{-}\mu\text{-}C_2Ph]_2$ (**4**),[6] a $(\mu\text{-}C_2Ph)_2$ structure (in principle D_{2h} or C_{2h} local symmetry seemed possible) such as A was suggested

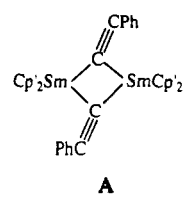

A

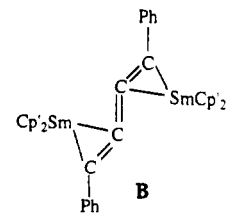

B

for compound **1**.[7] We were aware of an isomeric compound of structure B previously prepared from $Cp'_2Sm(THF)_2$ + PhC≡C—C≡CPh by Evans et al.[8] We discounted the possibility of this structure since the reported ^1H NMR spectrum[8] was distinctly different from what we found for

(1) For some examples involving olefins and acetylenes, see: (a) Molander, G. A.; Hoberg, J. O. *J. Am. Chem. Soc.* **1992**, *114*, 3123–3125. (b) Heeres, H. J.; Teuben, J. H. *Organometallics* **1991**, *10*, 1980–1986 and references therein. (c) Heeres, H. J.; Meetsma, A.; Teuben, J. H.; Rogers, R. D. *Organometallics* **1989**, *8*, 2637–2646. (d) Jeske, G.; Lauke, H.; Mauermann, H.; Swepston, P. N.; Schumann, H.; Marks, T. J. *J. Am. Chem. Soc.* **1985**, *107*, 8091–8103. (e) Jeske, G.; Schock, L. E.; Mauermann, H.; Swepston, P. N.; Schumann, H.; Marks, T. J. *J. Am. Chem. Soc.* **1985**, *107*, 8103–8110. (f) Jeske, G.; Lauke, H.; Mauermann, H.; Schumann, H.; Marks, T. J. *J. Am. Chem. Soc.* **1985**, *107*, 8111–8118. (g) Watson, P. L.; Parshall, G. W. *Acc. Chem. Res.* **1985**, *18*, 51–55.

(2) Manriquez, J. M.; Fagan, P. J.; Marks, T. J.; Vollmer, S. H.; Day, C. S.; Day, V. W. *J. Am. Chem. Soc.* **1979**, *101*, 5075–5078.

(3) Nolan, S. P.; Stern, D.; Marks, T. J. *J. Am. Chem. Soc.* **1989**, *111*, 7844–7853 and references therein.

(4) Atwood, J. L.; Hunter, W. E.; Wayda, A. L.; Evans, W. J. *Inorg. Chem.* **1981**, *20*, 4115–4119.

(5) Evans, W. J.; Bloom, I.; Hunter, W. E.; Atwood, J. L. *Organometallics* **1983**, *2*, 709–714.

(6) Boncella, J. M.; Tilley, T. D.; Andersen, R. A. *J. Chem. Soc., Chem. Commun.* **1984**, 710–712.

0276-7333/93/2312-3618$04.00/0

1. Since structures A and B are centrosymmetric isomers, they are not differentiable by elemental analysis, cryoscopy, or first-order ^{1}H NMR-derived symmetry information.

Subsequent to our report, Evans, Keyer, and Ziller (EKZ)[9] showed by diffraction that compound 1 (eq 3) actually has structure B in the solid state. Thus, eq 3 involves a new, lanthanide-mediated C—C bond-forming reaction. EKZ additionally asserted that an uncoupled dimeric structure such as A was sterically prohibited. Although they did not specifically propose a mechanism for the C—C bond formation, the only possibilities discussed were within the context of "oxidative coupling" and similar Ti chemistry thought to involve "internal reduction and oxidation" ($2Cp_2Ti—C\equiv CPh \rightarrow 2Cp_2Ti + PhC\equiv C—C\equiv CPh \rightarrow$ final product, eq 4).[10] Since Sm

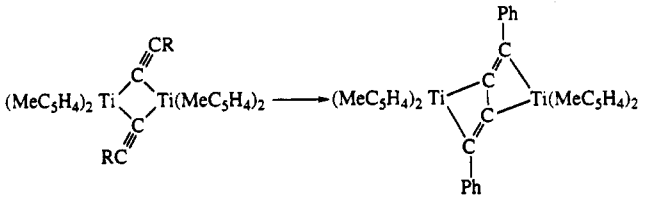

(4)

has both divalent and trivalent states accessible by organometallic transformations and since $Cp'_2Sm(THF)_2$ had previously been found to undergo reaction with $PhC\equiv C—C\equiv CPh$ to also yield B,[8] the possibility that Sm(III) → Sm(II) reductive elimination/ligand oxidative coupling occurs at some place along the eq 3 reaction coordinate might be a natural assumption. The possible role of dimeric precursors (cf. eq 4[10]) and phenyl-stabilized alkynyl/bis(alkynyl) anionic intermediates are also legitimate mechanistic issues.

In an attempt to shed further light on these mechanistic questions regarding eq 3, we focus here on three issues and their probes: (i) Is a redox-active lanthanide necessary for the facile coupling process? We investigate the diamagnetic (to assist NMR monitoring of reactions), non-redox-active metal ion La^{3+} [11] and demonstrate facile coupling. (ii) Can a dimer (e.g., A) lie along the reaction coordinate to B? We report the isolation, characterization, and smooth unimolecular conversion in solution of an uncoupled dimeric species to a B-type structure. (iii) Are π-delocalizing phenyl substituents essential for facile acetylene coupling? We illustrate that this is not the case using *tert*-butylacetylene moieties. In the process, we are also led to reassign the NMR spectrum of 1.

Experimental Section

Materials and Methods. The organolanthanide complexes described in this paper are rapidly decomposed in air. Consequently, all manipulations were carried out under an atmosphere of purified nitrogen or argon in a Vacuum Atmospheres glovebox or using standard high-vacuum (<10^{-5} Torr) techniques. Solvents were predried and distilled from appropriate drying agents, stored over Na/K alloy, and vacuum transferred to reaction vessels. ^{1}H NMR spectra were obtained on a Varian XL 400 (FT, 400 MHz, probe temperature ≈ 30 °C for ^{1}H spectroscopy) spectrometer. IR spectra were measured using a Perkin-Elmer 283 instrument and were calibrated with polystyrene. Elemental analyses were performed by Oneida Research Services, New York. Cryoscopic molecular weight measurements were determined in benzene using a Knauer Cryoscopic Unit which had been modified to work under strictly anaerobic conditions. The lanthanum alkyl $Cp'_2LaCH(SiMe_3)_2$ was prepared by the literature procedure.[1d] The alkynes PhCCH and *t*-BuCCH were dried over activated molecular sieves and then degassed and transferred to a storage container under vacuum.

Kinetic Measurements. In a typical kinetics experiment, a 5-mm NMR tube fitted with a Teflon valve (J. Young) was loaded with an accurately prepared solution of $(Cp'_2LaCC\text{-}t\text{-}Bu)_2$ in C_6D_6 containing 1% $CH_2(SiMe_3)_2$ as an internal standard. The NMR tube was inserted into the spectrometer and heated to the desired temperature, allowing approximately 1 min to reach thermal equilibrium, and then an initial spectrum (t = 0) was recorded. At appropriate time intervals, subsequent ^{1}H NMR spectra were recorded. The kinetics were monitored by following the integrated intensity of the starting Cp′ and/or *t*-Bu signals relative to the signals of the standard. Due to partial crystallization of the product during the experiment, no data were collected by following the appearance of the product Cp′ signal. The kinetics were monitored for at least 2-3 half-lives. The data for these reactions were fitted by least-squares analysis to $\ln(C_t/C_0) = kt$, where C_t is the concentration of $(Cp'_2LaCC\text{-}t\text{-}Bu)_2$ at time t, and C_0 is the initial concentration.

$(Cp'_2La)_2(\mu\text{-}PhC_4Ph)\cdot 2(toluene)$ (5). Under an argon flush, 60 μL (0.55 mmol) of PhCCH was syringed into a suspension of 0.32 g (0.56 mmol) of $Cp'_2LaCH(SiMe_3)_2$ in 15 mL of pentane at −78 °C. The reaction flask was allowed to warm to 0 °C over a period of 20 min and then was brought to room temperature. The volatile components were removed *in vacuo*, and the solid was extracted with 20 mL of toluene. After filtering, the solution volume was reduced to 10 mL and then slowly cooled to −78 °C. Red-brown crystals of $(Cp'_2La)_2(\mu\text{-}PhC_4Ph)\cdot 2PhMe$ were collected by cold filtration and dried *in vacuo*. Yield: 0.22 g (75%). ^{1}H NMR (C_6D_6, 20 °C): δ 7.27 (t, ^3J = 8 Hz, 2H, *m*-H), 7.03 (t, ^3J = 8 Hz, 1H, *p*-H), 6.78 (d, ^3J = 8 Hz, 2H, *o*-H), 2.08 (s, 30H, Cp′); peaks attributable to PhMe were observed at 7.14, 7.04, and 2.12 ppm. Samples undergo partial loss of lattice toluene upon drying under high vacuum. Anal. Calcd for $C_{56}H_{70}La_2\cdot{}^1/_2C_7H_8$: C, 66.97; H, 6.99. Found: C, 66.65; H, 6.78. Reaction of the product with D_2O gave $Ph_2C_4D_2$ by GC–MS (M^+ m/z 206).

$(Cp'_2La)_2(\mu\text{-}t\text{-}BuC_4\text{-}t\text{-}Bu)$ (6). Excess *t*-BuCCH was vacuum transferred onto a solution of 0.14 g (0.24 mmol) of $Cp'_2LaCH(SiMe_3)_2$ in 20 mL of toluene. The reaction mixture was left stirring at room temperature under argon for 2 h. The volatile components were then removed *in vacuo*, and the residue was dissolved in 15 mL of toluene and filtered, and the toluene solution was heated to 60 °C for 4 h. Orange-red crystals of $(Cp'_2La)_2(\mu\text{-}t\text{-}BuC_4\text{-}t\text{-}Bu)$ were collected by filtration and dried under high vacuum. Yield: 0.06 g (52%). ^{1}H NMR (C_6D_6, 20 °C): δ 2.07 (s, 30H, Cp′), 1.24 (s, 9H, *t*-Bu). IR (Nujol mull, cm^{-1}): 2725 (m), 1568 (m), 1302 (w), 1261 (m), 1231 (m), 1172 (w), 1151 (w), 1019 (m), 878 (m), 722 (s), 641 (m), 605 (m), 550 (m), 451 (m), 432 (m), 412 (m). Anal. Calcd for $C_{52}H_{78}La_2$: C, 63.67; H, 8.01. Found: C, 63.70; H, 8.00. Reaction of the product with D_2O gave $(t\text{-}Bu)_2C_4D_2$ by GCMS (M^+ m/z 166).

$(Cp'_2LaCC\text{-}t\text{-}Bu)_2$ (7). In a procedure similar to the above, excess *t*-BuCCH was reacted with 0.30 g (0.53 mmol) of $Cp'_2LaCH(SiMe_3)_2$ in 40 mL of pentane at 0 °C for 10 h. The volatiles were removed *in vacuo*, and the pale yellow residue was taken up in 40 mL of cold toluene. After filtration, the toluene solution was reduced and the supernatant decanted from the

(7) Although $\nu_{C\equiv CR}$ stretching modes are common signatures of metal acetylide functionalities, their absence (as in 1) does not constitute rigorous proof that such structures are not present. For an example where a $\nu_{C\equiv CR}$ mode could not be detected in a *bona fide* lanthanide acetylide complex, see: Evans, W. J.; Ulibarri, T. A.; Chamberlain, L. R.; Ziller, J. W.; Alvarez, D. A., Jr. *Organometallics* **1990**, *9*, 2124–2130.

(8) Evans, W. J.; Keyer, R. A.; Zhang, H.; Atwood, J. L. *J. Chem. Soc., Chem. Commun.* **1987**, 837–838.

(9) Evans, W. J.; Keyer, R. A.; Ziller, J. W. *Organometallics* **1990**, *9*, 2628–2631.

(10) (a) Sekutowski, D. G.; Stucky, G. D. *J. Am. Chem. Soc.* **1976**, *98*, 1376–1382. (b) See also: Cuenca, T.; Gomez, R.; Gomez-Sal, P.; Rodriguez, G. M.; Royo, P. *Organometallics* **1992**, *11*, 1229–1234 and references therein.

(11) (a) Thermodynamic estimates[11b] place aqueous $E°(Ln^{3+} \rightarrow Ln^{2+})$ at ~−3.74 V for Ln = La vs ~−1.57 V for Ln = Sm. (b) Morss, L. R. *Chem. Rev.* **1976**, *76*, 827–842.

Table I. Crystallographic Details

complex	$(Cp'_2La)_2(\mu\text{-}PhC_4Ph)\cdot 2PhMe$	$(Cp'_2La)_2(\mu\text{-}t\text{-}BuC_4\text{-}t\text{-}Bu)$
formula	$C_{70}H_{86}La_2$	$C_{52}H_{78}La_2$
MW	1205.20	981.00
space group	$C2/m$	$P2_1/n$ (No. 14)
a, Å	15.600(2)	11.232(2)
b, Å	14.318(2)	14.199(3)
c, Å	15.368(2)	15.309(4)
β, deg	114.17(1)	103.35(2)
vol, Å^3	3124.4(6)	2376(1)
Z	2	2
density (calcd), g cm^{-3}	1.281	1.371
cryst dimens, mm	0.28 × 0.32 × 0.40	0.2 × 0.3 × 0.4
radiation	Mo Kα	Mo Kα
linear abs coeff cm^{-1}	13.9	18.11
temp, K	296	153
scan mode	$\omega/2\theta$	$\omega/2\theta$
2θ limit, deg	48.0	54.0
scan range	4–48	2–54
no. of data collcd	2516	5671
no. of data observed	1815 ($I \geq 4\sigma(I)$)	4461 ($I > 2.58\sigma(I)$)
$R(F)$	0.050	0.027
$R(wF)$	0.063	0.034

precipitated product. Recrystallization by diffusion of pentane into a saturated toluene solution at −78 °C gave pale yellow crystals of $(Cp'_2LaCC\text{-}t\text{-}Bu)_2$ which were collected by filtration and dired *in vacuo*. Yield: 0.16 g (60%). ^{1}H NMR (toluene-d_8, 20 °C): δ 2.21 (s, 30H, Cp'), 1.27 (s, 9H, *t*-Bu). IR (Nujol mull, cm^{-1}): 2725 (m), 2020 (m), 1262 (w), 1213 (m), 1150 (w), 1085 (w), 1020 (m), 967 (w), 880 (w), 800 (m), 725 (m), 700 (w), 598 (w), 580 (m). Anal. Calcd for $C_{52}H_{78}La_2$ (MW, 981.0): C, 63.67; H, 8.01. Found (MW, 1100(±60)): C, 63.48; H, 7.78. Heating $(Cp'_2LaCC\text{-}t\text{-}Bu)_2$ in C_6D_6 resulted in the formation of $(Cp'_2La)_2(\mu\text{-}t\text{-}BuC_4\text{-}t\text{-}Bu)$ (^{1}H NMR identification) as the sole product.

$Cp'_2LaCC\text{-}t\text{-}Bu(THF)$. In a procedure similar to the above, excess *t*-BuCCH was reacted with 0.30 g (0.53 mmol) of $Cp'_2LaCH(SiMe_3)_2$ in 20 mL of THF at 0 °C for 12 h. The volatile components were removed *in vacuo*, and the white residue was taken up in 40 mL of pentane. After filtration, the pentane solution was reduced in volume to 10 mL and then slowly cooled to −78 °C. Cold filtration afforded $Cp'_2LaCC\text{-}t\text{-}Bu(THF)$ as colorless needles. Yield: 0.26 g (87%). ^{1}H NMR (C_6D_6, 20 °C): δ 3.48 (m, 4H, α-THF), 2.12 (s, 30H, Cp'), 1.41 (s, 9H, *t*-Bu), 1.18 (m, 4H, β-THF). IR (Nujol mull, cm^{-1}): 2725 (m), 2060 (m), 1354 (m), 1242 (s), 1021 (m), 1074 (w), 1017 (s), 946 (w), 915 (w), 860 (m br), 802 (w), 713 (m), 665 (w), 584 (w), 543 (w), 432 (m). Anal. Calcd for $C_{30}H_{47}LaO$ (MW, 562.6): C, 64.05; H, 8.42. Found (MW, 570(±60)): C, 64.17; H, 8.36. After $Cp'_2LaCC\text{-}t\text{-}Bu(THF)$ was heated in C_6D_6 for 48 h at 60 °C, no change in the ^{1}H NMR spectrum was observed.

X-ray Crystallographic Study of $(Cp'_2La)_2(\mu\text{-}PhC_4Ph)\cdot 2(toluene)$ (5). A red-brown specimen was grown from toluene solution and immediately mounted in a glass capillary. Diffraction data, 2516 independent reflections, 2θ scan range 4–48° (1815 independent observed $F_o \geq 4\sigma(F_o)$ reflections) were collected at 296 K using a Nicolet R3m diffractometer with Mo Kα radiation (λ = 0.710 73 Å). An empirical correction for absorption was applied to the reflection data. The crystal was found to be isomorphous with the previously reported Sm compound.[9] Non-hydrogen atomic coordinates from the Sm complex were used to initialize the refinement. All non-hydrogen atoms were anisotropically refined, and hydrogen atoms were treated as idealized contributions. The maximum shift/error Δ/σ(max) was 0.03, and the highest feature of the final difference Fourier map ranged from +0.78 to −1.71 e Å^{-3}. The structure was refined to ($R(F)$ = 0.050 and $R(wF)$ = 0.063. As in the previous structure, two molecules of toluene accompany each dinuclear complex. All computations and sources of scattering factors used SHELXTL (5.1) software (G. Sheldrick, Nicolet (Siemens), Madison, WI). Crystallographic details are complied in Table I, and atomic coordinates in Table II.

X-ray Crystallographic Study of $(Cp'_2La)_2(\mu\text{-}t\text{-}BuC_4\text{-}t\text{-}Bu)$ (6). An orange, translucent, platelike crystal was cut from a larger crystal grown from C_6D_6 solution, mounted using oil (paratone-N, Exxon), and then cooled to −120 °C. Diffraction data were measured on a Enraf-Nonius CAD4 diffractometer (ω/θ scan mode, ω scan angle = 1.50[1.00 + 0.35 tan(θ)]°) with Mo Kα radiation (λ = 0.701 73 Å); 5671 independent reflections were obtained ($2\theta_{max}$ = 54.0°), 4461 with $I > 2.58\sigma(I)$ being considered "observed". Corrections for Lorentz and polarization effects and anomalous dispersion were applied. A numerical absorption correction was applied; maximum and minimum transmission factors were 0.669 and 0.524, respectively. The structure was solved by direct methods (SHELXS-86); correct positions for all non-hydrogen atoms were deduced from an electron density map. Subsequent least-squares difference Fourier calculations revealed the positions for the hydrogen atoms. In the final cycle of least squares, anisotropic thermal coefficients were refined for the non-hydrogen atoms and isotropic thermal parameters were refined for the hydrogens. Successful convergence was indicated by the maximum shift/error, 0.13, for the last cycle. The highest peaks in the final difference Fourier ranged from +0.87 to −1.62 e Å^{-3} and were in the vicinity of the lanthanum position (SHELX-76). Final agreement factors were R = 0.027 and R_w = 0.034. Crystallographic details are compiled in Table I, and atomic coordinates in Table III.

Table II. Final Atomic Coordinates and Equivalent Isotropic Thermal Parameters for the Non-Hydrogen Atoms of $(Cp'_2La)_2(\mu\text{-}PhC_4Ph)$ (5)

atom	x	y	z	U_{eq} (Å^2)
La	0.05652(4)	0	0.1995.1(4)	0.599(3)
C1	−0.0976(9)	0	0.0462(8)	0.087(6)
C2	−0.0411(6)	0	−0.0016(7)	0.059(4)
C3	−0.2040(7)	0	0.0005(10)	0.084(6)
C4	−0.2529(10)	0	0.0531(12)	0.142(10)
C5	−0.3492(14)	0	0.0145(14)	0.155(13)
C6	−0.3945(10)	0	−0.0774(13)	0.128(9)
C7	−0.3425(16)	0	−0.1316(12)	0.175(13)
C8	−0.2509(9)	0	−0.0872(11)	0.121(9)
C9	0.0967(12)	0.1906(7)	0.2094(8)	0.118(7)
C10	0.1600(7)	0.1546(8)	0.3012(8)	0.107(5)
C11	0.1042(9)	0.1327(8)	0.3480(6)	0.112(6)
C12	0.0125(7)	0.1495(8)	0.2904(8)	0.105(6)
C13	0.0055(8)	0.1864(8)	0.2054(8)	0.104(5)
C14	0.1326(18)	0.2277(11)	0.1379(12)	0.320(23)
C15	0.2633(7)	0.1470(12)	0.3403(13)	0.216(11)
C16	0.1373(20)	0.1120(11)	0.4536(8)	0.325(20)
C17	0.0653(11)	0.1411(14)	0.3222(14)	0.242(17)
C18	0.0702(12)	0.2302(9)	0.1261(10)	0.224(11)
Cs1	0.6887(19)	0	0.2851(14)	0.272(25)
Cs2	0.6585(31)	0	0.3232(16)	0.350(34)
Cs3	0.6005(16)	0.0842(12)	0.3438(12)	0.213(12)
Cs4	0.5395(16)	0.0822(28)	0.3780(17)	0.398(30)
Cs5	0.5035(17)	0	0.3993(19)	0.340(30)

Results and Discussion

Synthesis of Coupled and Uncoupled Lanthanum Alkynyl Complexes. The addition of PhC≡CH to a stirring pale yellow pentane solution of $Cp'_2LaCHTMS_2$ at room temperature results in a rapid color change to red-brown. Evaporation of the solvent, extraction of the product into toluene, and crystallization at −78 °C afford $(Cp'_2La)_2(\mu\text{-}PhC_4Ph)$ (**5**) in 75% isolated yield as a toluene solvate (as the only NMR-detectable product, eq 5). The

$$2Cp'_2LaCHTMS_2 + 2PhC{\equiv}CH \rightarrow \underset{\mathbf{5}}{(Cp'_2La)_2(\mu\text{-}PhC_4Ph)} + 2TMS_2CH_2 \quad (5)$$

product was characterized by elemental analysis and standard spectroscopic techniques (it crystallizes with two toluene molecules per formula unit—see Experimental Section for details). Consistent with the presence of a

Table III. Final Atomic Coordinates and Equivalent Isotropic Thermal Parameters for the Non-Hydrogen Atoms of $(Cp'_2La)_2(\mu\text{-}t\text{-}BuC_4\text{-}t\text{-}Bu)$ (6)

atom	x	y	z	U_{eq} (Å^2)
La	0.04003(1)	0.99375(1)	0.82902(1)	0.01219(9)
C1	0.2765(3)	1.0488(2)	0.8152(2)	0.019(1)
C2	0.2003(3)	1.0754(2)	0.7314(2)	0.022(1)
C3	0.1275(3)	1.1519(2)	0.7464(2)	0.022(1)
C4	0.1603(3)	1.1740(2)	0.8395(2)	0.018(1)
C5	0.2526(3)	1.1102(2)	0.8817(2)	0.016(1)
C6	0.3754(3)	0.9746(3)	0.8264(3)	0.024(2)
C7	0.2199(4)	1.0449(3)	0.6418(2)	0.047(2)
C8	0.0408(4)	1.2064(3)	0.6753(3)	0.036(2)
C9	0.1229(3)	1.2606(2)	0.8827(3)	0.029(2)
C10	0.3223(3)	1.1154(3)	0.9776(2)	0.032(2)
C11	−0.1896(3)	0.9069(2)	0.7471(2)	0.015(1)
C12	−0.1140(3)	0.8330(2)	0.7899(2)	0.019(1)
C13	−0.0197(3)	0.8190(2)	0.7428(2)	0.017(1)
C14	−0.0397(3)	0.8838(2)	0.6705(2)	0.019(1)
C15	0.1433(3)	0.9393(2)	0.6737(2)	0.021(1)
C16	−0.3127(3)	0.9322(3)	0.7639(3)	0.016(2)
C17	−0.1372(4)	0.7742(3)	0.8656(2)	0.037(2)
C18	0.0776(3)	0.7445(3)	0.7615(3)	0.027(2)
C19	0.0196(4)	0.8763(3)	0.5922(2)	0.037(2)
C20	−0.2038(4)	1.0112(2)	0.6054(2)	0.039(2)
C21	0.0430(3)	0.9665(2)	1.0081(2)	0.017(1)
C22	0.1227(3)	0.9098(2)	0.9853(2)	0.016(1)
C23	0.2028(3)	0.8421(2)	1.0505(2)	0.016(1)
C24	0.1767(3)	0.8487(2)	1.1448(2)	0.024(2)
C25	0.3384(3)	0.8653(2)	1.0581(3)	0.017(2)
C26	0.1804(3)	0.7404(2)	1.0175(2)	0.034(2)

μ-PhC_4Ph functionality, treatment of **5** with D_2O, followed by GC—MS of the volatile products yields $Ph_2C_4D_2$. As will be seen below, X-ray diffraction reveals that complex **5** has structure B and is metrically rather similar to **1** (*vide infra*). Clearly, a redox-active lanthanide center is not required for the C–C coupling process.

In contrast to the results of eq 5, $Cp'_2LaCC\text{-}t\text{-}Bu(THF)$ does not undergo NMR-detectable coupling after heating for 48 h at 60 °C. Similar observations were obtained for the Sm analogue,[9] where the necessity of heating at 125 °C for prolonged periods to produce **1** could indicate a mechanistically dissimilar coupling pathway.[12]

The reaction of $Cp'_2LaCHTMS_2$ with t-BuC≡CH is somewhat slower than eq 5; however heating at 60 °C for 4 h results in quantitative conversion to bright orange $(Cp'_2La)_2(\mu\text{-}t\text{-}BuC_4\text{-}t\text{-}Bu)$ (**6**, eq 6). This new complex was

$$2Cp'_2LaCHTMS_2 + 2t\text{-}BuC{\equiv}CH \rightarrow \underset{\mathbf{6}}{2(Cp'_2La)_2(\mu\text{-}t\text{-}BuC_4\text{-}t\text{-}Bu)} + 2TMS_2CH_2 \quad (6)$$

characterized by standard spectroscopic techniques and elemental analysis. Reaction of **6** with D_2O yields $(t\text{-}Bu)_2C_4D_2$ by GC–MS. Further confirmation of the C—C coupled structure is provided by diffraction results (*vide infra*) which indicate that **6** possesses a μ-t-BuC=C=C=C-t-Bu configuration qualitatively similar but quantitatively dissimilar to **5** in metrical parameters. Clearly, aryl functionalization is not a necessary condition for the coupling process to occur, although it may effect some kinetic acceleration.

If the reaction of eq 6 is carried out at 0 °C, it is possible to isolate another product in 60% yield. Elemental analysis, NMR, and solution cryoscopic molecular weight are consistent with a second, dimeric complex of empirical formula $(Cp'_2LaC_2\text{-}t\text{-}Bu)_2$ (**7**). In the infrared, **7** exhibits a $\nu_{C\equiv C\text{-}t\text{-}Bu}$ stretching frequency at 2020 cm^{-1}, which can be compared to reported μ-C≡C-t-Bu values of 2050 cm^{-1} (**2**),[4] 2035 cm^{-1} (**3**),[5] and 2050 cm^{-1} for $[(CH_3C_5H_4)_2Yb\text{-}\mu\text{-}C{\equiv}C\text{-}t\text{-}Bu]_2$[4] and 2036 cm^{-1} for $[(t\text{-}BuC_5H_4)_2Sm\text{-}\mu\text{-}C{\equiv}CPh]_2$.[14] In comparison, terminal $\nu_{C\equiv C\text{-}t\text{-}Bu}$ stretches for metals of the same mass generally occur at somewhat higher energies: 2060 cm^{-1} for $Cp'_2La(THF)C{\equiv}C\text{-}t\text{-}Bu$ (see Experimental Section) and 2072 cm^{-1} for $Cp'_2Sm(THF)C{\equiv}C\text{-}t\text{-}Bu$.[7] Further evidence that the acetylide units of **7** have not undergone coupling is provided by deuterolysis experiments, which produce only t-BuCCD by GC–MS. Efforts to grow crystals of **7** suitable for diffraction studies have so far been unsuccessful. In the absence of these data, rigorous definition of the molecular structure cannot be made, however, a μ-C≡C-t-Bu structure such as A (D_{2h} or distorted, C_{2h} local symmetry) is one dimeric possibility consistent with the spectroscopic data. Interestingly, the solution ^{1}H NMR spectrum of **7** is temperature-dependent, with the Cp′ signal reversibly shifting 0.16 ppm upfield on increasing the temperature from 20 to 80 °C in toluene-d_8. This may be indicative of reversible disassociation–reassociation of the structure and is also evident in the **7** → **6** reaction kinetics (*vide infra*). The ^{1}H spectrum gives no evidence of broadening down to −80 °C in toluene-d_8.

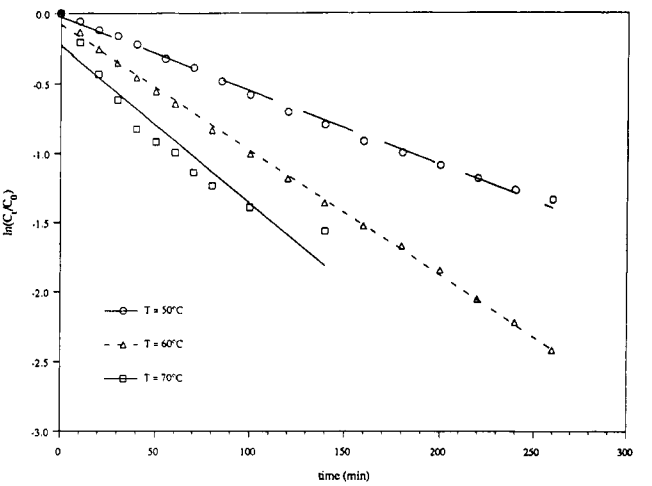

Figure 1. First-order kinetic plots for the thermal conversion of $(Cp'_2LaC{\equiv}C\text{-}t\text{-}Bu)_2$ (**7**) to $(Cp'_2La)_2(\mu\text{-}t\text{-}BuC_4\text{-}t\text{-}Bu)$ (**6**) in toluene-d_8 solution: T − 50 °C, C_0 = 0.0095 M, k = 0.0052 min^{-1} (R = 0.999); T = 60 °C, C_0 = 0.0050 M, k = 0.0089 min^{-1} (R = 0.999); T = 70 °C, C_0 = 0.0020 M, k = 0.0113 min^{-1} (R = 0.957).

Conversion of a Dimeric Acetylide 7 to μ-C_4R_4 Complex 6. The kinetics of the conversion of **7** → **6** were monitored by NMR over 2–3 half-lives. The data evidence clean **7** → **6** conversion with no evidence of intermediates or side reactions, although partial precipitation of **6** occurs at higher concentrations/longer reaction times. As can be seen in Figure 1, the kinetic data taken at 50 and 60 °C exhibit clean first-order kinetics for the C–C coupling reaction. At 70 °C, significant deviations from first-order kinetics are observed (Figure 1); such behavior would be consistent with increasing bimolecular character as the extent of the dissociation of **7** increases. Importantly, these

(12) See also: Keyer, R. A.; Ziller, J. W.; Evans, W. J. *Abstr. Pap.—Am. Chem. Soc.* **1992**, *203*, INOR 671. $Cp'_2Ln(THF)C{\equiv}CPh$ complexes (Ln = Ce, Nd) are also reported to yield coupling products under unspecified conditions.

(13) Atwood, J. L.; Hunter, W. E.; Wayda, A. L.; Evans, W. J. *Inorg. Chem.* **1981**, *20*, 4115–4119.

(14) Shen, Q.; Zheng, D.; Lin, L.; Lin, Y. *J. Organomet. Chem.* **1990**, *391*, 307–312.

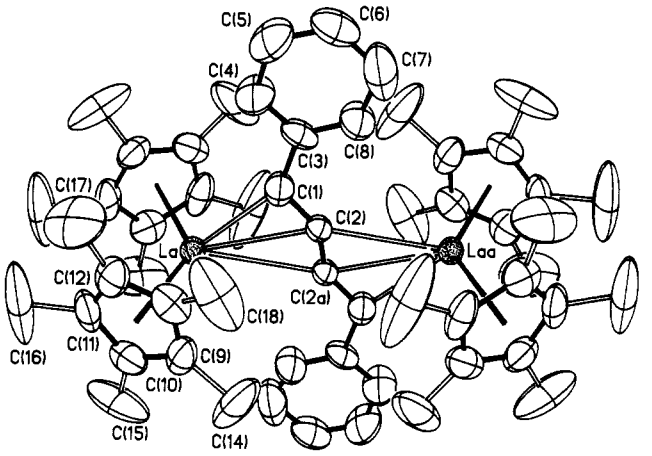

Figure 2. ORTEP plot (35% probability ellipsoids) of the molecular structure of $(Cp'_2La)_2(\mu\text{-}PhC_4Ph)\cdot 2PhMe$ (**5**). The lattice toluene molecules and the hydrogen atoms have been omitted for clarity. Symmetry-equivalent atoms are designated by an "a".

Table IV. Selected Bond Lengths (Å) and Angles (deg) in $(Cp'_2La)_2(\mu\text{-}RC_4R)$

R = Ph (**5**)		R = *t*-Bu (**6**)	
	Bond Lengths		
La–C1	2.577(10)	La–C22	2.642(3)
La–C2	2.823(9)	La–C21	2.761(3)
La–C2(a)	2.950(11)	La–C21′	2.912(3)
av La–C(Cp)	2.80(2)	av La–C(Cp)	2.85(3)
La–Cp(cent)	2.540(5)	La–Cp(cent)	2.587(3), 2.583(3)
C1–C2	1.36(2)	C21–C22	1.310(4)
C2–C2(a)	1.26(2)	C21–C21′	1.338(4)
C1–C3	1.51(2)	C22–C23	1.521(4)
	Bond Angles		
Cp(cent)–La–Cp–(cent)	133.1(3)	Cp(cent)–La–Cp(cent)	132.99(9)
C1–C2–C2(a)	148.6(13)	C22–C21–C21′	153.7(3)
C2–C1–C3	125.6(11)	C21–C22–C23	123.4(3)

kinetic results argue that dimer **7** is the direct kinetic precursor of the C–C coupled, μ-RC_4R complex **6**.

Molecular Structures of $(Cp'_2La)_2(\mu\text{-}RC_4R)$ Where R = Ph and *t*-Bu. Single crystal X-ray analysis of **5** (Figure 2) reveals that this complex is isostructural with the Sm analogue (structure B). Selected bond lengths and angles are listed in Table IV. The molecular structure and atom labeling scheme are shown in Figure 2. Although most La–C bond distances directly reflect the differences in La^{3+} and Sm^{3+} ionic radii (0.081 Å for eight-coordination,[14] neither La–C2 nor La–C2(a) exhibit such expansions (2.823(9) vs 2.807(8) and 2.950(11) vs 2.963(9) Å, respectively). The reasons probably reflect the slightly more open La^{3+} coordination sphere (allowing closer approach), and the fact that these long contacts represent relatively weak interactions. The present La–C1 distance of 2.577(10) Å can be compared to La–C σ bond lengths of 2.537(5) and 2.588(4) Å in $Cp'La(CHTMS_2)_2$,[16] 2.651 (8) and 2.627(10) Å in $Cp'La(CHTMS_2)_2THF$,[16] and 2.633(4) Å in $Cp'_2La(THF)(\mu\text{-}\eta^1,\eta^3\text{-}C_4H_6)LaCp'_2$.[17] The parameters associated with the present La–Cp′ bonding are unexceptional, as are those within the μ-PhC_4Ph fragment.

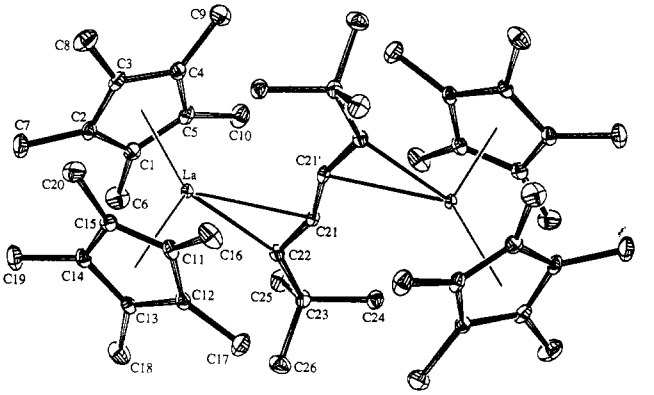

Figure 3. ORTEP plot (35% probability ellipsoids) of the molecular structure of $(Cp'_2La)_2(\mu\text{-}t\text{-}BuC_4\text{-}t\text{-}Bu)$ (**6**). The hydrogen atoms have been omitted for clarity.

Selected bond distances and angles for $(Cp'_2La)_2(\mu\text{-}t\text{-}BuC_4\text{-}t\text{-}Bu)$ (**6**) are also given in Table IV. The overall molecular geometry (Figure 3) is similar to that in **5**; however the bonding to the coupled acetylene fragment is significantly more symmetrical. Thus, La–C22 = 2.642(3) Å is longer than the corresponding distance in **5** (2.577(10) Å), while La–C21 = 2.761(3) Å is shorter than the corresponding distance in **5** (2.823(9) Å). Furthermore, La–C21′ = 2.912(3) Å is shorter than the corresponding distance in **5** (2.950(11) Å). Within the C_4 fragment, the pronounced bond alternation observed in **5** (C1–C2 = 1.36(2), C2–C2(a) = 1.26(2) Å) is diminished in **6** (corresponding distances: C22–C21 = 1.310(4), C21–C21′ = 1.338(4) Å). Again, the metrical parameters associated with the Cp'_2La fragment of **6** are unexceptional.

Reassignment of the ^{1}H NMR Spectrum of Compound 1. Evans et al. reported ^{1}H spectral features (assignments) for **1** in THF-d_8 as follows: δ 9.29, doublet, J = 7.5 Hz (*o*-H); 5.87, broad triplet, J = 5 Hz (*p*-H); 4.98, multiplet (*m*-H); 1.36, singlet (Cp′). Our initial studies in toluene-d_8 could not reproduce the δ 9.29 signal and instead placed the *o*-H resonance at δ 2.12, a feature which we now suspect to be the toluene of solvation, unknown to us at the time. It should be noted that the chemical shifts of paramagnetic organolanthanides[18] are typically more sensitive to temperature and solvent than the diamagnetic analogues. We have now reexamined the ^{1}H spectrum of **1** as concentrated solutions in toluene-d_8 and THF-d_8. The spectra have been assigned with the aid of 1-D decoupling. The following assignments are confirmed in THF-d_8: δ 5.89, broad multiplet (*m*-H); 5.82, triplet, J = 8.0 Hz (*p*-H); 1.29, singlet (Cp′); −5.13, broad (*o*-H). The following assignments are confirmed in toluene-d_8: δ 5.29, triplet, J = 7.6 Hz, (*p*-H); 3.90, broad multiplet (*m*-H); 1.36, singlet (Cp′); −10.2, broad (*o*-H).

Conclusions

These results demonstrate that chemical excursion between formal lanthanide oxidation states +2 and +3 is not required to mediate the facile acetylide fusion process of eq 3. That is, metal reductive elimination/ligand

(15) Shannon, R. D. *Acta Crystallogr.* **1976**, *A32*, 751–767.
(16) van der Heijden, H.; Schaverien, C. J.; Orpen, A. G. *Organometallics* **1989**, *8*, 255–258.
(17) Scholz, A.; Smola, A.; Scholz, J.; Loebel, J.; Schumann, H.; Thiele, K. H. *Angew. Chem., Int. Ed. Engl.* **1991**, *30*, 435–436.
(18) (a) Fischer, R. D. In *Organometallics of the f-Elements*; Marks, T. J., Fischer, R. D., Eds.; Reidel: Dordrecht, The Netherlands, 1979; Chapter 11. (b) Fischer, R. D. In *Fundamental and Technological Aspects of Organo-f-Element Chemistry*; Marks, T. J., Fragala, I. L., Eds.; Reidel: Dordrecht, The Netherlands, 1985; Chapter 8. (c) Bertini, I.; Luchinat, C. *NMR of Paramagnetic Molecules in Biological Systems*, Benjamin: Menlo Park, CA, 1986; Chapter 10.

oxidative coupling[9,10] need not be invoked. Furthermore, this reaction is not restricted to arylacetylenes, and the immediate kinetic precursor of coupled product **6** is an uncoupled dimer (**7**). Beyond these facts, the exact mechanism is open to speculation, with both "concerted" (eq 7, essentially a valence isomerization) and "insertive"

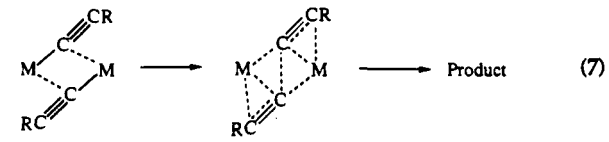

(7)

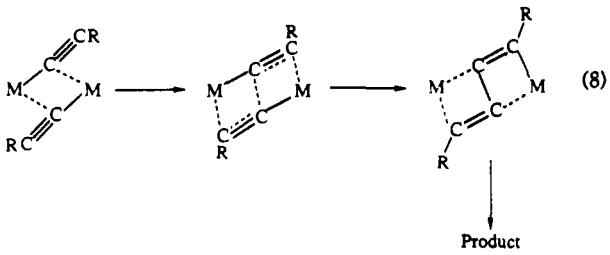

(8)

(eq 8) pathways accommodating the present information. In terms of bonding energetics, it is apparent that the C—C bond formation, attendant π delocalization, and the multihapto metal—C bond formation accrued in assembling the μ-RC_4R product enthalpically outweigh the loss of M—C≡CR bonding (estimated from U/Sm bond enthalpy proportionalities[3] to be ~90 kcal/mol for M = Sm) and C≡C bonding (~70 kcal/mol) in the starting material. Whether or not the lanthanide—C bonds have significant polar character is clearly not an inhibitor of the present coupling process.

Note Added in Proof. Subsequent to submission and acceptance of this manuscript for publication, two related contributions have appeared from the groups of Teuben and Evans. Heeres, Nijhoff, Teuben, and Rogers (*Organometallics* **1993**, *12*, 2609–2617) describe the synthesis, characterization, and reactions of the R = CH_3, *t*-Bu (Ln = Ce) and R = CH_3 (Ln = La) analogues of the present complexes. Spectral and structural data are in agreement with the present results. In regard to the C—C coupling process, these authors present evidence that the uncoupled and coupled R = CH_3 (Ln = La) species are in slow, virtually temperature-independent equilibrium ($\Delta H \approx -1$ kcal/mol). The approach to equilibrium/C—C coupling could be modeled kinetically as a first-order process, in agreement with the present R = *t*-Bu (Ln = La) results. However, we observed no evidence for such an equilibrium in our system, and the curved 70 °C kinetic plot in our Figure 1 is not suggestive of a simple first-order approach to equilibrium (nor is the difference from the 50 and 60 °C plots if $\Delta S = 0$). The observation that the $\Delta G/\Delta H$ difference between the coupled and uncoupled structures is so small is completely consistent with our earlier bond disruption enthalpy analysis.[3] Evans, Keyer, and Ziller (*Organometallics* **1993**, *12*, 2618–2633) report a synthesis, characterization, and reactivity study of a series of Ce, Nd, and Sm acetylide complexes. Relevant to the present mechanistic discussion, further examples are reported of $Cp'_2Ln(THF)C{\equiv}CPh$ complexes which undergo the C—C coupling reaction under drastic conditions. The crystal structure of a weakly linked dimer, $(Cp'_2SmC_2\text{-}t\text{-}Bu)_2$, is also reported. While it may be structurally related to the present complex **7** of the larger La^{3+} ion (and Teuben's complexes **3**, **4**, and **5** of Ce^{3+} and La^{3+}), this is difficult to judge in the absence of necessary analytical, infrared, NMR, and solution molecular weight data.

Acknowledgment. We thank the NSF for support of this research under Grant CHE9104112.

Supplementary Material Available: Tables of X-ray experimental details including crystal data, positional and anisotropic displacement parameters, and bond lengths and angles (33 pages). Ordering information is given on any current masthead page.

OM9301804